

## Quasi-elastic and massive transfer reactions in the $^{16}\text{O} + ^{89}\text{Y}$ reaction at beam energies around $\approx 4\text{--}5$ MeV/nucleon

R. Tripathi,<sup>1</sup> S. Sodaye,<sup>1</sup> K. Mahata,<sup>2</sup> and P. K. Pujari<sup>1</sup><sup>1</sup>Radiochemistry Division, Bhabha Atomic Research Centre, Mumbai-400 085, India<sup>2</sup>Nuclear Physics Division, Bhabha Atomic Research Centre, Mumbai-400 085, India

(Received 16 April 2014; revised manuscript received 23 July 2014; published 28 August 2014)

Kinetic energy spectra, angular distributions, and cross sections of projectilelike fragments (PLFs) with  $Z_{\text{PLF}} = 3\text{--}7$  have been measured in  $^{16}\text{O} + ^{89}\text{Y}$  reaction at  $E_{\text{lab}} = 62.2, 73.4, 78.5,$  and  $83.5$  MeV respectively. Comparison of angular distributions of PLFs, particularly of nitrogen (N), at different beam energies showed increasing contribution from overlapping collision trajectories at higher beam energies. Angular distributions of PLFs became more forward peaked with the amount of mass transfer indicating an increasing overlap of the projectile and the target nuclei with increasing mass transfer. PLF cross sections could be reasonably explained by the modified sum-rule model except for carbon (C) indicating the role of alpha cluster structure of  $^{16}\text{O}$  nucleus in the transfer process. Large cross section for PLF emitted in the  $\alpha$  transfer channel in  $^{16}\text{O} + ^{89}\text{Y}$  reaction compared to that in  $^{19}\text{F} + ^{89}\text{Y}$  reaction further supported this observation.

DOI: 10.1103/PhysRevC.90.027604

PACS number(s): 25.70.Hi

Reactions involving incomplete mass transfer such as quasi-elastic transfer (QET) and massive transfer or incomplete fusion (ICF) have been an active area of investigation for a long time. Several models such as sum-rule model [1,2], overlap model [3–6], break-up fusion model [7–9] and multi-step direct reaction theory [10] were proposed to explain these reactions. In the studies by Morgenstern *et al.* [11,12], the probability of incomplete fusion reaction was related to the entrance channel mass asymmetry. However, these models hold good at beam energies of about  $\sim 10$  MeV/nucleon and above. At even higher beam energies ( $\gtrsim 15$  MeV/nucleon), it has been shown that incomplete mass transfer reactions have contribution from projectile break-up and coalescence of nucleons during nucleon-nucleon interaction [13–18]. At lower beam energies ( $\sim 5$  MeV/nucleon), the mechanism of incomplete mass transfer is not well understood, particularly the contribution from collision trajectories with different impact parameters as a function of beam energy. Several studies have been carried out in the recent past to investigate the reactions involving incomplete mass transfer at lower beam energies [19–25]. At energies very close to the entrance channel Coulomb barrier, such reactions are dominated by quasi-elastic transfer (QET) of a few nucleons [26,27]. Kinetic energy spectra of projectilelike fragments (PLFs) formed in QET peak at an optimum  $Q$  value i.e.,  $Q_{\text{opt}}$  decided by the kinematics of the reaction [28]. In QET dissipative effects are negligible. On the other hand in deep inelastic collisions (DIC), projectile and targetlike products appear at energies corresponding to the exit channel Coulomb barrier. The transition from QET to DIC represents a shift in the reaction mechanism and massive transfer or incomplete fusion reactions lie in-between these two extremes in terms of impact parameter and kinetic energy dissipation. In the studies by Mermaz *et al.* in  $^{19}\text{F} + ^{89}\text{Y}$  reaction at  $E_{\text{lab}} = 140$  MeV [29], it was shown that the full kinetic energy dissipation takes place at larger angles even for PLFs with  $Z$  close to that of the projectile. This suggests that even PLFs formed following small mass transfer have contribution from dissipative reaction mechanisms at higher

beam energies. In spite of extensive studies, contribution from different reaction mechanisms to the formation of PLFs in the lower energy domain ( $\sim 5$  MeV/nucleon) has remained a less explored subject. It is important to investigate the evolution of the reaction mechanism involved in the formation of PLFs which changes from purely grazing to overlapping collisions with increasing beam energy.

Apart from the beam energy, projectile structure also plays an important role in the reactions involving incomplete mass transfer [30–32]. For projectiles with  $\alpha$  cluster structure, cross sections for even  $Z$  PLFs have been observed to be higher than that of the neighboring odd  $Z$  PLFs [30]. Such structure effects have also been observed in the cross sections of evaporation

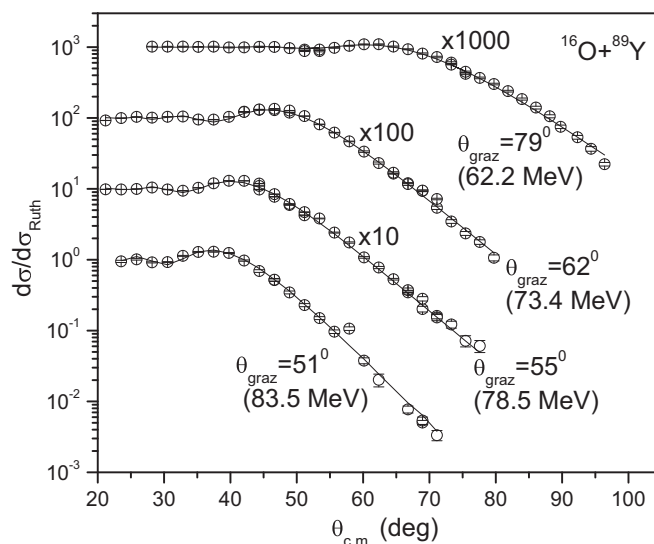


FIG. 1. Plot of elastic scattering data at different beam energies for  $^{16}\text{O} + ^{89}\text{Y}$  system. Solid lines are fit to the data using the code SNOOPY 8Q [33]. Grazing angle values in center of mass frame of reference are given in the figure. The values inside the bracket are corresponding beam energies.

TABLE I. Optical model parameters obtained from the fitting of elastic scattering data using the code SNOOPY 8Q [33].

$E_{\text{lab}}$ (MeV)	$V$ (MeV)	$R_0$ (fm)	$a_0$ (fm)	$W$ (MeV)	$R_{i,0}$ (fm)	$a_{i,0}$ (fm)	$\sigma_{\text{Total}}$ (mb)
62.2	78.40	1.182	0.556	23.50	1.099	0.828	1586
73.4	75.90	1.250	0.448	24.61	1.179	0.476	2160
78.5	89.78	1.269	0.416	24.53	1.186	0.535	2544
83.5	90.50	1.230	0.457	26.06	1.182	0.405	2655

residues (ERs) [19,31,32]. In the off-line radiochemical measurement of cross sections of evaporation residues in  $^{16}\text{O} + ^{89}\text{Y}$  reaction by Tomar *et al.* [32], enhancement in the cross sections of Rh ( $Z = 45$ ) and Nb ( $Z = 41$ ) isotopes with respect to the statistical model values was observed to be much larger compared to that in the case of other evaporation residues. Such an enhancement may be attributed to the preferential transfer of an  $\alpha$  particle or  $^{12}\text{C}$  to the target nucleus because of the favorable  $Q$  values of the transfer reactions or projectile break-up into  $^4\text{He} + ^{12}\text{C}$ . However, more importantly, there may be an additional effect due to the projectile cluster structure which may enhance the cross section for transfer of  $^4\text{He}$  or  $^{12}\text{C}$ . A quantitative comparison of cross sections of PLFs or ERs from reactions induced by

projectiles with and without  $\alpha$  cluster structure can help in disentangling the effect of  $Q$  value and  $\alpha$  cluster structure of the projectile. For example, the  $Q$  value for the break-up of  $^{16}\text{O}$  ( $^{16}\text{O} \rightarrow ^4\text{He} + ^{12}\text{C}$ ) and  $^{19}\text{F}$  ( $^{19}\text{F} \rightarrow ^4\text{He} + ^{15}\text{N}$ ) are  $-7.2$  and  $-4.0$  MeV respectively. Also, if the  $Q$  value for the transfer of  $\alpha$  particle to the target is to be considered, the typical values for a target nucleus, e.g.,  $^{89}\text{Y}$  are  $-5.23$  and  $-2.09$  MeV for  $^{16}\text{O}$  and  $^{19}\text{F}$  induced reactions respectively. Thus, a comparison of the cross section for  $^4\text{He}$  transfer in the two reactions can give information about the role played by the cluster structure in the transfer process.

In order to investigate the evolution of the reaction mechanism with beam energy and the role of  $\alpha$  cluster structure of the projectile, angular distributions and cross sections of projectilelike fragments with  $Z_{\text{PLF}} = 3-7$  have been measured in  $^{16}\text{O} + ^{89}\text{Y}$  reaction at  $E_{\text{lab}} = 62.2, 73.4, 78.5,$  and  $83.5$  MeV respectively. Elastic scattering measurements have been carried out at these beam energies to get information about the grazing angle and normalization of cross section data. The present results on PLF cross sections have been compared with those from our earlier measurements in  $^{19}\text{F} + ^{89}\text{Y}$  reaction [23] to investigate the role of  $\alpha$  cluster structure. The PLF cross section data from the present measurements have been compared with the calculations of modified sum-rule model [1,2,22].

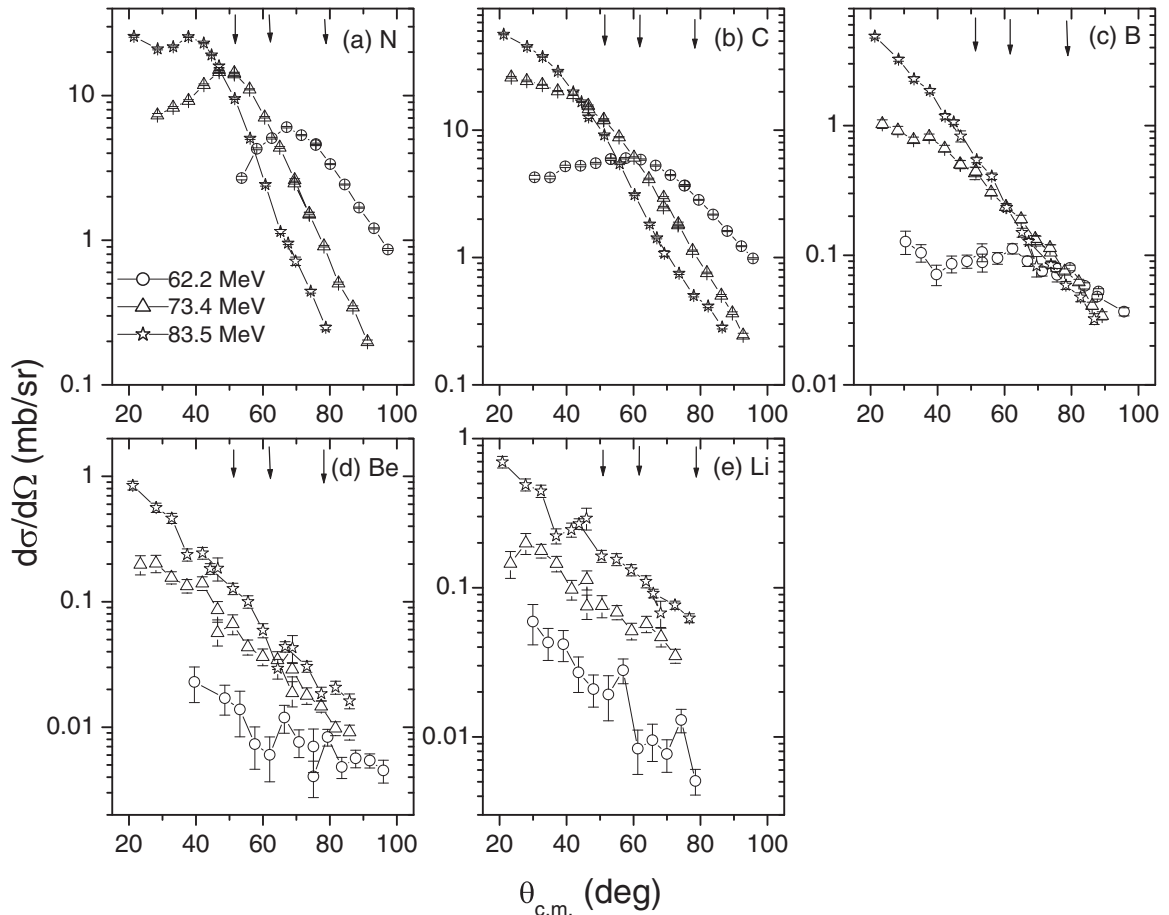


FIG. 2. Angular distribution of different projectilelike fragments (PLFs) formed in  $^{16}\text{O} + ^{89}\text{Y}$  reaction at various beam energies. In each panel, arrows from right to left mark the grazing angles corresponding to  $E_{\text{lab}} = 62.2, 73.4,$  and  $83.5$  MeV respectively.

Experiments were carried out at BARC-TIFR Pelletron-LINAC facility at Tata Institute of Fundamental Research, Mumbai, India. A self-supporting target of  $^{89}\text{Y}$  (thickness  $1.1\text{ mg/cm}^2$ ) was mounted at the center of a scattering chamber of 1 m diameter. The target was mounted at  $\sim 30^\circ$  with respect to the beam direction. PLFs and elastically scattered beam particles were detected using three silicon detector based  $E$ - $\Delta E$  telescopes, which were mounted on a movable arm. Angular distributions were measured in the range  $\theta_{\text{lab}} = 18$ – $86^\circ$ . Two monitor detectors were mounted at  $\pm 20^\circ$  with respect to the beam direction. Data were acquired using a multiparameter data acquisition system with continuous monitoring of the dead time. Count rates of elastic peaks in the monitor detectors were used to normalize the data of the telescopes for the beam current and target thickness to obtain absolute cross sections.

Figure 1 shows the plot of elastic scattering data in  $^{16}\text{O} + ^{89}\text{Y}$  reaction at different beam energies. The ratio of experimental cross section to Rutherford scattering cross section ( $d\sigma/d\sigma_{\text{Ruth}}$ ) at forward angles was normalized to unity and the normalization factors were used to normalize the PLF cross sections. Elastic scattering data were fitted using the code SNOOPY 8Q [33]. Fitted curves are shown as solid lines in Fig. 1 and the fit parameters are given in Table I. Center of mass (CM) grazing angles obtained from fitting of the elastic scattering data are given in Fig. 1.

Center of mass angular distributions of PLFs with  $Z_{\text{PLF}} = 3$ – $7$  for  $E_{\text{lab}} = 62.2$ ,  $73.4$ , and  $83.5$  MeV are shown in Fig. 2.

Data for  $E_{\text{lab}} = 78.5$  MeV are not shown in the figure for the sake of clarity of the figure. Beam energy dependence of the angular distribution of N shows that it is predominantly formed in grazing collision trajectories at the lowest beam energy (peaking close to the grazing angle). With increasing beam energy, contribution from overlapping collisions increases as seen from the forward peaking of the angular distribution at  $E_{\text{lab}} = 83.5$  MeV. Angular distribution at  $E_{\text{lab}} = 78.5$  MeV was also similar. Angular distributions of C are nearly similar to those of N, peaking close to the grazing angle at lowest beam energy and becoming forward peaked with increasing beam energy. For B, Be, and Li, angular distributions are forward peaked even at the lowest beam energy. As in the case of beam energy dependence, forward peaking of angular distributions with increasing mass transfer indicates the increasing effect of attractive nuclear force, arising from the increasing overlap of the projectile and the target nuclei.

Cross sections of different PLFs were obtained from the respective plots of “ $(d\sigma/d\Omega) \cdot 2\pi \sin(\theta_{\text{c.m.}})$  vs  $\theta_{\text{c.m.}}$ ”. The plots for B, C, and N showed a deviation from the Gaussian distribution as expected from their angular distributions shown in Fig. 2. Therefore, cross sections for these PLFs were determined by the extrapolation to  $0$  and  $180^\circ$ , which was governed by the first two and the last two data points at the extreme ends of the angular distributions. In the case of lighter PLFs, the uncertainties on the individual data points were large. Therefore, such an extrapolation procedure was not reliable.

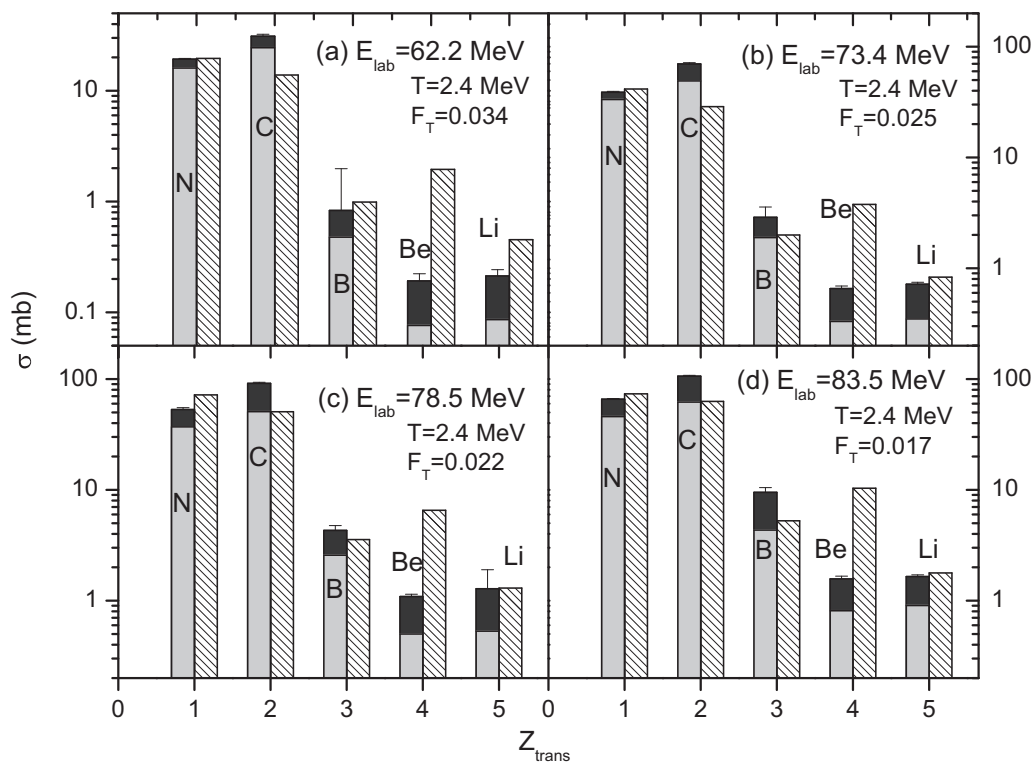


FIG. 3. Cross sections of projectilelike fragments in  $^{16}\text{O} + ^{89}\text{Y}$  reaction at  $E_{\text{lab}} = 62.2$  MeV (a),  $73.4$  MeV (b),  $78.5$  MeV (c), and  $83.5$  MeV (d). Abscissa represents amount of charge transferred ( $Z_{\text{trans}}$ ). Bars are labeled with the corresponding PLFs. Filled bars are the experimental data (light grey: cross section corresponding to the angular range covered in the measurement; dark grey: cross section obtained by extrapolation/fitting). Bars with pattern (slanting lines) are the results of modified sum-rule model calculations. The parameter  $T$  and  $F_T$  obtained from the fit are also given in the figure (see text for details).

Hence, in the case of Be and Li, angular distributions were fitted to Gaussian function. In the fitting, the centroid of the Gaussian was kept fixed at  $0^\circ$  as an approximation as there was a continuous increase in the cross sections at forward angles making the peak position uncertain. The cross sections of PLFs at different beam energies are shown in Fig. 3. The light and dark grey portions of the bars represent, respectively, the cross sections corresponding to the angular region covered in the experiment and cross section obtained by extrapolation/fitting. The uncertainties shown in the figure are due to extrapolation or fitting. It should be mentioned here that there may be additional uncertainty due to the assumption of monotonous nature of angular distribution while extrapolation or peaking of Gaussian function at  $0^\circ$  during fitting. However, as a substantial part of the cross sections comes from the measured angular distribution, such uncertainties are not expected to be large enough to affect the conclusions of the present study.

For comparison, cross sections of PLFs were calculated using the modified sum-rule model [1,2,22], which allows effective contribution to incomplete fusion from  $l$ -waves lower than  $l_{\text{crit}}$  for complete fusion [34]. The modified sum-rule model reasonably explained the cross section for reactions involving incomplete mass transfer at these low beam energies [22], which were otherwise underestimated. In the cross section calculation by the original sum-rule model,  $R_C$  (radius parameter governing the internuclear separation at which transfer occurs),  $T$  (effective temperature), and  $\Delta$  (diffuseness of  $l$  distribution) are adjustable parameters [1,2]. In the modified sum-rule model  $F_T$  is an additional empirical parameter which makes transmission coefficient dependent on number of transferred nucleons for  $l < l_{\text{crit}}$  [22]. In the present calculations, the values of  $R_C$  and  $\Delta$  were taken as 1.5 fm and  $0.3\hbar$  respectively, as used in Refs. [1,2]. Parameters  $T$  and  $F_T$  were obtained from the best fit to the data as judged by the  $\chi^2$ . The results of modified sum-rule model calculations are shown in Fig. 3 by bars with slanting lines. Calculated cross sections of PLFs having the same  $Z$  but different  $A$  were added for comparison with experimental values. The values of  $T$  and  $F_T$  obtained from the fit are also given in the figure. The modified sum-rule model calculations reasonably explained the cross sections of PLFs except for C and Be where the deviation was very large, though in opposite directions. The large calculated values for Be compared to the experimental values may be attributed to the underestimation of Be yield due to the break-up of  $^8\text{Be}$  into two  $\alpha$  particles. For C, it can be seen from Fig. 3 that calculated cross sections are substantially lower (almost by a factor of  $\sim 2$ ) compared to the experimental values. As  $Q$  values for different transfer channels are used as input in the calculation, the observed enhancement of the experimental cross section of C above the calculated values indicates the role of  $\alpha$  cluster structure which would enhance the formation of  $^{12}\text{C}$ .

In order to further investigate the role of cluster structure, PLF cross section data from the present measurement have been compared with those from  $^{19}\text{F} + ^{89}\text{Y}$  reaction. PLF cross section data from  $^{16}\text{O} + ^{89}\text{Y}$  and  $^{19}\text{F} + ^{89}\text{Y}$  reactions are shown as a function of  $E_{\text{c.m.}}/V_b$  ( $E_{\text{c.m.}}$  is the energy in c.m. frame of reference and  $V_b$  is the entrance channel Coulomb barrier) in Fig. 4. For comparison, cross section data of PLFs

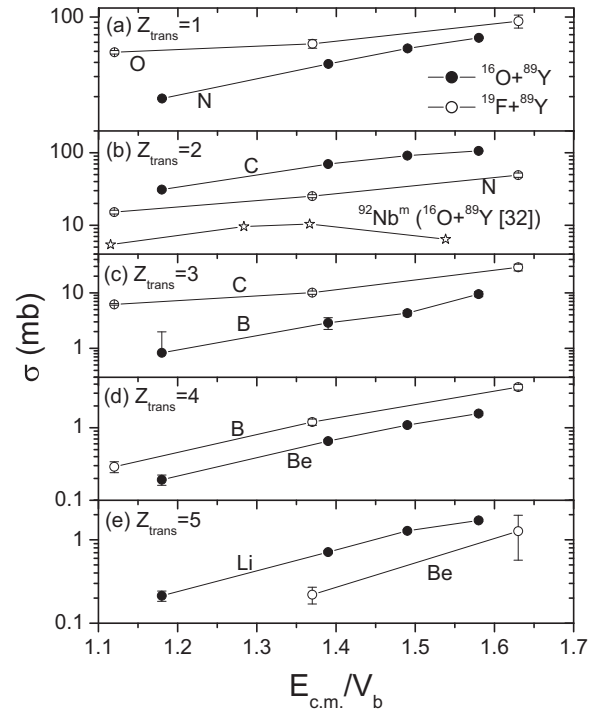


FIG. 4. Comparison of cross sections of projectilelike fragments (PLFs) from  $^{16}\text{O} + ^{89}\text{Y}$  and  $^{19}\text{F} + ^{89}\text{Y}$  reactions, plotted as a function of  $E_{\text{c.m.}}/V_b$ . Cross sections corresponding to the different amount of charge transfer ( $Z_{\text{trans}}$ ) are shown in different panels. Evaporation residue data for  $Z_{\text{trans}} = 2$  from Ref. [32] are also shown in the figure.

formed in the transfer channels involving the same amount of charge transfer ( $Z_{\text{trans}}$ , where  $Z_{\text{trans}}$  is the amount of charge transferred) are shown in the same panel. The cross section data from the two reaction systems have been directly compared as total reaction cross sections for the two systems would be similar at a given value of  $E_{\text{c.m.}}/V_b$ . It can be seen from this figure that PLF cross sections for all the transfer channels are higher in  $^{19}\text{F} + ^{89}\text{Y}$  reaction compared to the respective values in  $^{16}\text{O} + ^{89}\text{Y}$  reaction except for  $Z_{\text{trans}} = 2$  and 5, for which the trend is reversed. In general, the larger cross section values in  $^{19}\text{F} + ^{89}\text{Y}$  reaction may be due to the larger value of  $l_{\text{max}}$  in this reaction at a given value of  $E_{\text{c.m.}}/V_b$  compared to that in  $^{16}\text{O} + ^{89}\text{Y}$  reaction. The case of  $Z_{\text{trans}} = 5$  is not important as it corresponds to emission of Be in  $^{19}\text{F} + ^{89}\text{Y}$  reaction which is underestimated due to break-up of  $^8\text{Be}$ . For  $Z_{\text{trans}} = 2$ , the cross section is much larger (by a factor of about  $\sim 2$ ) in  $^{16}\text{O} + ^{89}\text{Y}$  reaction compared to that in  $^{19}\text{F} + ^{89}\text{Y}$ . This observation clearly indicates the role of  $\alpha$  cluster structure of  $^{16}\text{O}$  nucleus in the transfer process. The cross section of the evaporation residue  $^{92}\text{Nb}^m$  corresponding to  $Z_{\text{trans}} = 2$  from Ref. [32] is also shown in the figure for comparison. The lower cross section values for  $^{92}\text{Nb}^m$  may be due to the fact that it is the low spin isomer and the high spin isomer  $^{92}\text{Nb}^g$ , which is expected to be the major product, could not be detected because of its long half-life.

In summary, angular distributions and cross sections of projectilelike fragments were measured to get information about

the evolution of incomplete mass transfer mechanism with beam energy and amount of mass transfer. Angular distributions of PLFs, particularly of N, become more forward peaked with increasing beam energy, indicating the contribution from collision trajectories with deeper interpenetration of the projectile and the target nuclei even for transfer channels involving only a few nucleons. Also, angular distributions of PLFs become more forward peaked with increasing mass transfer.

PLF cross sections (Be excluded) were reasonably explained by the modified sum-rule model calculations except for C. In the case of C, calculated cross sections were lower

by a factor of about  $\sim 2$ . A comparison of cross sections of PLFs corresponding to  $Z_{\text{trans}} = 2$  in  $^{16}\text{O} + ^{89}\text{Y}$  and  $^{19}\text{F} + ^{89}\text{Y}$  reactions showed larger cross sections (by a factor of about  $\sim 2$  or more) in the case of the former even though the  $Q$  value for  $\alpha$  transfer channel is less negative in the latter case. These observations indicate the role played by the  $\alpha$  cluster structure of the projectile nucleus in the transfer process.

We are thankful to Dr. S. K. Sharma and Dr. P. Maheshwari for their help during the experiment. We would like to thank Dr. A. Goswami and Dr. K. Sudarshan for valuable discussions.

- 
- [1] J. Wilczynski, K. Siwek-Wilczynska, J. Van Driel, S. Gonggrijp, D. C. J. M. Hageman, R. V. F. Janssens, J. Lukasiak, R. H. Siemssen, and S. Y. Van Der Werf, *Nucl. Phys. A* **373**, 109 (1982).
- [2] K. Siwek-Wilczynska, E. H. du Marchie van Voorthuysen, J. van Popta, R. H. Siemssen, and J. Wilczynski, *Phys. Rev. Lett.* **42**, 1599 (1979).
- [3] B. G. Harvey, *Nucl. Phys. A* **444**, 498 (1985).
- [4] B. G. Harvey and M. J. Murphy, *Phys. Lett. B* **130**, 373 (1983).
- [5] Adel Y. Abul-Magd, *Z. Phys. A* **298**, 143 (1980).
- [6] M. H. Simbel and A. Y. Abul-Magd, *Z. Phys. A* **294**, 277 (1980).
- [7] T. Udagawa and T. Tamura, *Phys. Rev. Lett.* **45**, 1311 (1980).
- [8] T. Udagawa and T. Tamura, *Phys. Lett. B* **116**, 311 (1982).
- [9] E. Takada, T. Shimoda, N. Takahashi, T. Yamaya, K. Nagatani, T. Udagawa, and T. Tamura, *Phys. Rev. C* **23**, 772 (1981).
- [10] V. I. Zagrebaev, *Ann. Phys. (NY)* **197**, 33 (1990).
- [11] H. Morgenstern, W. Bohne, W. Galster, K. Grabisch, and A. Kyanowski, *Phys. Rev. Lett.* **52**, 1104 (1984).
- [12] H. Morgenstern, W. Bohne, W. Galster, and K. Grabisch, *Z. Phys. A* **324**, 443 (1986).
- [13] E. Gadioli *et al.*, *Nucl. Phys. A* **708**, 391 (2002).
- [14] E. Gadioli *et al.*, *Eur. Phys. J. A* **17**, 195 (2003).
- [15] L. J. Mudau *et al.*, *Nucl. Phys. A* **761**, 190 (2005).
- [16] B. Becker *et al.*, *Eur. Phys. J. A* **18**, 639 (2003).
- [17] E. Z. Buthelezi, F. Cerutti, E. Gadioli, G. F. Steyn, A. Pepe, S. H. Connell, and A. A. Cowley, *Eur. Phys. J. A* **28**, 193 (2006).
- [18] E. Z. Buthelezi, F. Cerutti, E. Gadioli, G. F. Steyna, S. H. Connell, and A. A. Cowley, *Nucl. Phys. A* **753**, 29 (2005).
- [19] K. Kumar, T. Ahmad, S. Ali, I. A. Rizvi, A. Agarwal, R. Kumar, K. S. Golda, and A. K. Chaubey, *Phys. Rev. C* **87**, 044608 (2013).
- [20] A. Yadav, V. R. Sharma, P. P. Singh, R. Kumar, D. P. Singh, Unnati M. K. Sharma, B. P. Singh, and R. Prasad, *Phys. Rev. C* **86**, 014603 (2012).
- [21] R. Ali, D. Singh, M. Afzal Ansari, M. H. Rashid, R. Guin, and S. K. Das, *J. Phys. G* **37**, 115101 (2010).
- [22] R. Tripathi, K. Sudarshan, S. Sodaye, A. V. R. Reddy, A. Goswami, B. K. Nayak, and S. K. Sharma, *Phys. Rev. C* **79**, 064604 (2009).
- [23] R. Tripathi, K. Sudarshan, S. Sodaye, and A. Goswami, *J. Phys. G* **35**, 025101 (2008).
- [24] A. Kumar, R. Tripathi, S. Sodaye, K. Sudarshan, and P. K. Pujari, *Eur. Phys. J. A* **49**, 1 (2013).
- [25] A. Kumar, K. Sudarshan, S. Sodaye, R. Tripathi, and P. K. Pujari, *Int. J. Mod. Phys. E* **20**, 2305 (2011).
- [26] B. K. Nayak, R. K. Choudhury, D. C. Biswas, L. M. Pant, A. Saxena, D. M. Nadkarni, and S. S. Kapoor, *Phys. Rev. C* **55**, 2951 (1997).
- [27] D. C. Biswas, R. K. Choudhury, B. K. Nayak, D. M. Nadkarni, and V. S. Ramamurthy, *Phys. Rev. C* **56**, 1926 (1997).
- [28] Mermaz *et al.*, *Nucl. Phys. A* **441**, 129 (1985).
- [29] M. C. Mermaz, T. Suomuärvi, R. Lucas, B. Berthier, J. Matuszek, J. P. Coffin, G. Guillaume, B. Heusch, F. Jundt, and F. Rami, *Nucl. Phys. A* **456**, 186 (1986).
- [30] R. Tripathi, K. Sudarshan, S. Sodaye, S. K. Sharma, A. V. R. Reddy, and A. Goswami, *Eur. Phys. J. A* **42**, 25 (2009).
- [31] K. Surendra Babu, R. Tripathi, K. Sudarshan, B. D. Srivastava, A. Goswami, and B. S. Tomar, *J. Phys. G* **29**, 1011 (2003).
- [32] B. S. Tomar, A. Goswami, A. V. R. Reddy, S. K. Das, P. P. Burte, S. B. Manohar, and S. Prakash, *Z. Phys. A* **343**, 223 (1992).
- [33] P. Schwandt, SNOOPY Computer Programme: Optical Potential Model Code for Elastic Scattering Analysis, Indiana University Cyclotron Report, 1988.
- [34] J. Wilczynski, *Nucl. Phys. A* **216**, 386 (1973).